



Ref.TH.2213-CERN

A STUDY OF THE MULTIPLICITIES
ASSOCIATED WITH LARGE TRANSVERSE MOMENTUM PARTICLES

J. Abad and A. Cruz

Departamento de Fisica Teorica
Facultad de Ciencias, Universidad de Zaragoza

and

J.L. Alonso *)

CERN - Geneva.

A B S T R A C T

Recent experimental data on multiplicities in large transverse momentum reactions are analyzed in a two-jet picture whose features are previously fixed by data on inclusive cross-sections and correlations. Special attention has been devoted to the P_T and \sqrt{s} behaviour of the particle multiplicities at the ISR energy range. A particular result is that changes in the behaviour of the associated multiplicity may be a sharp signal of a fundamental transition in the dynamics of particle production.

*) Permanent address : Departamento de Fisica Teorica, Facultad de Ciencias, Universidad de Zaragoza, Spain.

Ref.TH.2213-CERN

23 August 1976

1. INTRODUCTION

A large number of different experimental groups¹⁻⁷⁾ have considered the reactions $pp \rightarrow hX$ for different hadrons h with large transverse momentum p_T . They have obtained data on inclusive cross-sections, correlations, and associated charged particle multiplicities. Although most of these data have not been analysed in detail, it has been shown⁸⁻¹⁰⁾ that the most outstanding features are well described by a two-jet picture. This two-jet picture could be considered as a general description of the hard collision without referring to specific models¹¹⁾.

The Pisa-Stony Brook¹²⁾ (PSB) data of charged particle multiplicities in both hemispheres associated with a large transverse momentum π^0 at 90° , for five different ISR energies, have been studied by this experimental group. They deduce⁷⁾ the charged multiplicity in a supposed jet on the away side. The jet multiplicity they found for $0.75 \text{ GeV}/c \leq p_T^{\pi^0} \leq 4.25 \text{ GeV}/c$ is interesting for two reasons: i) They find the associated average multiplicity growing almost linearly with $p_T^{\pi^0}$. This fact is compatible with the decay of a jet¹³⁾. ii) The average multiplicity, even after allowance for neutrals, means that the average p_T in the compensating mechanism is of $\sim 1 \text{ GeV}/c$ per particle. The ACHM data¹⁾ for $\sqrt{s} = 53 \text{ GeV}$ are in agreement with this estimate. This could imply the presence of hard processes in the $p_T^{\pi^0}$ regions analysed by the PSB Collaboration.

In the present work we study the PSB data on both hemispheres in a two-jet picture, whose features are previously fixed by data on inclusive cross-sections and correlations, taking into account trigger-bias. To be more specific, we assume that at small $p_T^{\pi^0}$ ($0 \text{ GeV}/c \leq p_T^{\pi^0} \leq 0.5 \text{ GeV}/c$) the production is dominantly "soft"¹¹⁾, while for large $p_T^{\pi^0}$ ($p_T^{\pi^0} \geq 1 \text{ GeV}/c$) it is dominantly hard and we can therefore use any of the quoted two-jet pictures⁸⁻¹⁰⁾ to analyse the multiplicity data.

As we shall explain in Section 2, we will take the specific two-jet picture of Refs. 8 and 13. In that section we will introduce an expression for the multiplicity associated with both jets and shall extend the necessary results of Refs. 8 and 13 to $1 \text{ GeV}/c < p_T^{\pi^0} < 2.5 \text{ GeV}/c$. In Section 3 we will discuss the multiplicity associated with the soft production and with the background (the residual set of particles not involved in the assumed jets). We will also analyse qualitatively the behaviour of the PSB data. This analysis is very important in order to support our assumption that at $p_T^{\pi^0} \approx 1 \text{ GeV}/c$ we have already the hard dynamics as the dominant one. In Section 4 we present the results of the fit to the PSB data of the multiplicities given by the chosen two-jet picture, whose essential features have been previously fixed. Section 5 contains a discussion of our results, and the conclusions.

2. TWO-JET PICTURE AND EXPRESSION FOR THE JET MULTIPLICITIES

In general, the associated mean charged multiplicity in each hemisphere [towards (t) and away (a) the trigger] for $p(p_1) + p(p_2) \rightarrow h(p_3) + X$, $\bar{n}^{t,a}(p_3)$, will receive contributions from pure hard and soft collision and from the interference of both. In this paper we shall consider only the cases in which one of them is assumed dominant.

We shall write $\bar{n}_s^{t,a}(p_3)$ [$\bar{n}_h^{t,a}(p_3)$] for the average charged multiplicity in the towards or in the away hemisphere associated with the soft (hard) collision.

Before evaluating $\bar{n}_h^{t,a}(p_3)$ we shall describe the two-jet picture we are going to use for the hard scattering. In the analysis of the cross-section and correlation data of Refs. 8 and 13, much attention has been devoted to the trigger bias. As the trigger bias is an important ingredient in our picture, "our jets" will be those of these references.

Although some strong assumptions and simplifications have been made in these papers in order to obtain analytical expressions to compare with data^{*}), their description is good enough to think that the information that is so far available does not allow a much more refined analysis.

They parametrize the cross-section for the production of a pair of jets of almost equal and opposite transverse momenta P_x in the form

$$\frac{d\sigma^{jet}}{dP_x} \equiv \Phi(P_x, \sqrt{s}) = \frac{A}{P_x^{m-1}} \quad (1)$$

Now, in the range $2.5 \text{ GeV}/c < p_T^{\pi^0} < 6 \text{ GeV}/c$, data from ACHM¹⁾ (for example) fit quite well, for each energy, to an inverse power of p_T , $(A'/p_T^{n_{eff}-1})$, with A' and n_{eff} essentially independent of p_T (we write $n-1$, $n_{eff}-1$ to leave n , n_{eff} for the invariant cross-section). It is easy to show, assuming scaling for $F^h(y)$, that a sufficient condition for the above-mentioned constancy of A' and n_{eff} is that A and n should be constant for each energy when $P_x > 2.5 \text{ GeV}/c$, and this will be assumed in this paper.

It has been shown^{8,13)}, that a good fit to present data on correlations can be obtained by supposing that both jets are described by the following fragmentation function

*) Scaling hypothesis for the fragmentation function of the jet $F^h(y)$; average over the jet masses and their possible different quantum numbers of the p_T dependence of the jets' cross-section and $F^h(y)$.

$$F^\pi(y) = B^\pi \frac{(1-y)^2}{y} + L_\rho + K^\pi \delta(y-1) \quad (2)$$

$(0 < y \leq 1)$

with coefficients

$$B^\pi \approx 0.6, \quad L_\rho \approx K^\pi \approx 0.01$$

which are approximately independent of the pion charge.

From Eqs. (1) and (2), the cross-section for the inclusive production of a large p_T pion is

$$\frac{d\sigma^\pi}{d^3p_x} = 2 \int_{\frac{p_x}{\sqrt{s}}}^{\sqrt{s}/2} \frac{dP_x}{P_x} \phi(P_x, \sqrt{s}) F^\pi(p_x/P_x), \quad (3)$$

and for $p_x > 2.5$ GeV/c

$$\approx \frac{2A}{p_x^{m-1}} \left[\frac{2B^\pi}{m(m-1)(m-2)} + \frac{L_\rho}{m-1} + K^\pi \right], \quad (4)$$

where p_x is the transverse momentum of the pion. Also from Eqs. (1) and (2) the average jet momentum $\langle P_x \rangle$, expected when one observes a large p_x pion is given by

$$r \equiv \frac{\langle P_x \rangle}{p_x} = \frac{\int_{\frac{p_x}{\sqrt{s}}}^{\sqrt{s}} dP_x \phi(P_x, \sqrt{s}) F^\pi(p_x/P_x)}{\int_{\frac{p_x}{\sqrt{s}}}^{\sqrt{s}} \frac{dP_x}{P_x} \phi(P_x, \sqrt{s}) F^\pi(p_x/P_x)}, \quad (5)$$

and for $p_x > 2.5$ GeV/c

$$\approx \frac{\frac{2B^\pi}{(m-1)(m-2)(m-3)} + \frac{L_\rho}{m-2} + K^\pi}{\frac{2B^\pi}{m(m-1)(m-2)} + \frac{L_\rho}{m-1} + K^\pi} \quad (6)$$

The r values given by formula (6) for different values of n , together with the energy at which each n is the approximately constant n_{eff} for $p_x^\pi > 2.5$ GeV/c, are given in Table 1. When $1 \text{ GeV/c} \lesssim p_x^\pi \lesssim 2.5 \text{ GeV/c}$, the hypothesis of the constancy of n_{eff} does not work and therefore formula (6) is not valid. In fact, both the BS Collaboration data²⁾ for π^\pm and those of the ACHM¹⁾ Collaboration for π^0 , give n_{eff} close to 5 when $p_x^\pi \sim 1 \text{ GeV/c}$. As the value of r is one of the ingredients in our work, we are going to discuss our estimate of r for $1 \text{ GeV/c} \lesssim p_x^\pi \lesssim 2.5 \text{ GeV/c}$.

We have considered two possibilities:

i) To begin with, we have taken, for each energy, the r value of Table 1 even for $1 \text{ GeV/c} \lesssim p_x^\pi \lesssim 2.5 \text{ GeV/c}$. To explain this choice, we are going to assume that r is a smooth function of p_T and that its values are not too big in this p_T region^{*}). In fact, naively, we would expect that at \sqrt{s} fixed ($p_T > 1 \text{ GeV/c}$) the changes of r with p_T would be comparable to its changes with \sqrt{s} (or n) at $p_T > 2.5 \text{ GeV/c}$ (see Table 1), because the changes of n_{eff} are similar in both cases. Besides, as we shall see in Section 3, we would expect, for p_x^π close to 1 GeV/c , that the behaviour of $\bar{n}_h^{t,a}$ with p_x^π would be dominated by the need of a threshold energy to produce the jets. Then, small changes of r would affect this threshold energy only a little, and not the general p_T behaviour of the data. It is only when we are far enough in p_T that the energy dependence of r will play, as we shall show, an interesting role. Briefly, we do not think that this choice will sensitively affect our results.

ii) One way to take into account the dependence on p_T of A and n is to write

$$\Phi(p_x, \sqrt{s}) \propto p_x \frac{\left(1 - \frac{2p_x}{\sqrt{s}}\right)^F}{(p_x^2 + M^2)^H} \quad (7)$$

This expression is suggested by the CIM¹⁴⁾. Then a method of extrapolating the r values of Ref. 13 to $p_x^\pi < 2.5 \text{ GeV/c}$ will be the following: If we assume scaling for $F^\pi(y)$ for $p_x^\pi > 1 \text{ GeV/c}$, using formulae (2) and (7) we can fit (3) to the ACHM cross-section data for $p_x^{\pi^0} > 1 \text{ GeV/c}$ and determine the parameters of (7). As in this work we are not interested in testing any model for the Φ distribution, but our wish is to take into account the A and n dependence with p_T , we have fitted each energy independently. However, as we have many parameters, in order to have

*) We can give the following well-known argument (see, for instance, Refs. 8 and 9): we know that the dynamics are such that transverse momentum is hard to produce and therefore it is "uneconomical" to produce "parents" with much more transverse momentum than is actually needed by the trigger.

$$F^\pi(y) = B^\pi \frac{(1-y)^2}{y} + L_\rho + K^\pi \delta(y-1) \quad (2)$$

$(0 < y \leq 1)$

with coefficients

$$B^\pi \approx 0.6, \quad L_\rho \approx K^\pi \approx 0.01$$

which are approximately independent of the pion charge.

From Eqs. (1) and (2), the cross-section for the inclusive production of a large p_T pion is

$$\frac{d\sigma^\pi}{d^3p_x} = 2 \int_{\frac{1}{p_x}}^{\sqrt{s}/2} \frac{dP_x}{P_x} \phi(P_x, \sqrt{s}) F^\pi(p_x/P_x), \quad (3)$$

and for $p_x > 2.5 \text{ GeV}/c$

$$\approx \frac{2A}{p_x^{m-1}} \left[\frac{2B^\pi}{m(m-1)(m-2)} + \frac{L_\rho}{m-1} + K^\pi \right], \quad (4)$$

where p_x is the transverse momentum of the pion. Also from Eqs. (1) and (2) the average jet momentum $\langle P_x \rangle$, expected when one observes a large p_x pion is given by

$$r \equiv \frac{\langle P_x \rangle}{p_x} = \frac{\int_{\frac{1}{p_x}}^{\sqrt{s}} dP_x \phi(P_x, \sqrt{s}) F^\pi(p_x/P_x)}{\int_{\frac{1}{p_x}}^{\sqrt{s}} \frac{dP_x}{P_x} \phi(P_x, \sqrt{s}) F^\pi(p_x/P_x)}, \quad (5)$$

and for $p_x > 2.5 \text{ GeV}/c$

$$\approx \frac{\frac{2B^\pi}{(m-1)(m-2)(m-3)} + \frac{L_\rho}{m-2} + K^\pi}{\frac{2B^\pi}{m(m-1)(m-2)} + \frac{L_\rho}{m-1} + K^\pi} \quad (6)$$

The r values given by formula (6) for different values of n , together with the energy at which each n is the approximately constant n_{eff} for $p_x > 2.5$ GeV/c, are given in Table 1. When $1 \text{ GeV/c} \lesssim p_x^\pi \lesssim 2.5 \text{ GeV/c}$, the hypothesis of the constancy of n_{eff} does not work and therefore formula (6) is not valid. In fact, both the BS Collaboration data²⁾ for π^\pm and those of the ACHM¹⁾ Collaboration for π^0 , give n_{eff} close to 5 when $p_x^\pi \sim 1 \text{ GeV/c}$. As the value of r is one of the ingredients in our work, we are going to discuss our estimate of r for $1 \text{ GeV/c} \lesssim p_x^\pi \lesssim 2.5 \text{ GeV/c}$.

We have considered two possibilities:

i) To begin with, we have taken, for each energy, the r value of Table 1 even for $1 \text{ GeV/c} \lesssim p_x^\pi \lesssim 2.5 \text{ GeV/c}$. To explain this choice, we are going to assume that r is a smooth function of p_T and that its values are not too big in this p_T region^{*}). In fact, naively, we would expect that at \sqrt{s} fixed ($p_T > 1 \text{ GeV/c}$) the changes of r with p_T would be comparable to its changes with \sqrt{s} (or n) at $p_T > 2.5 \text{ GeV/c}$ (see Table 1), because the changes of n_{eff} are similar in both cases. Besides, as we shall see in Section 3, we would expect, for p_x^π close to 1 GeV/c , that the behaviour of $\bar{n}_h^{t,a}$ with p_x^π would be dominated by the need of a threshold energy to produce the jets. Then, small changes of r would affect this threshold energy only a little, and not the general p_T behaviour of the data. It is only when we are far enough in p_T that the energy dependence of r will play, as we shall show, an interesting role. Briefly, we do not think that this choice will sensitively affect our results.

ii) One way to take into account the dependence on p_T of A and n is to write

$$\Phi(p_x, \sqrt{s}) \propto p_x \frac{\left(1 - \frac{2p_x}{\sqrt{s}}\right)^F}{(p_x^2 + M^2)^N} \quad (7)$$

This expression is suggested by the CIM¹⁴⁾. Then a method of extrapolating the r values of Ref. 13 to $p_x^\pi < 2.5 \text{ GeV/c}$ will be the following: If we assume scaling for $F^\pi(y)$ for $p_x^\pi > 1 \text{ GeV/c}$, using formulae (2) and (7) we can fit (3) to the ACHM cross-section data for $p_x^{\pi^0} > 1 \text{ GeV/c}$ and determine the parameters of (7).

As in this work we are not interested in testing any model for the Φ distribution, but our wish is to take into account the A and n dependence with p_T , we have fitted each energy independently. However, as we have many parameters, in order to have

*) We can give the following well-known argument (see, for instance, Refs. 8 and 9): we know that the dynamics are such that transverse momentum is hard to produce and therefore it is "uneconomical" to produce "parents" with much more transverse momentum than is actually needed by the trigger.

a feeling of a "physical" parametrization for Φ ¹¹⁾ we have chosen fits with $3 \leq N \leq 4.5$ and $M \sim 1$ GeV. The χ^2 of our fits are less than one per point. Table 2 sums up our result. Once we know the N, F, and M parameters, Eq. (5) gives Table 3 for $p_x^{\pi^0} > 1$ GeV/c.

As we see, our assumption (i) about r is confirmed by this second method. However, at the lowest ISR energies (23 and 31 GeV) the r values change suddenly between $p_x^{\pi^0} = 1.75$ and $p_x^{\pi^0} = 1.25$. This effect could be caused by our extrapolation method. In fact, the assumption of scaling for $p_x^{\pi^0} > 1$ GeV/c is probably wrong. Also, the multiplicities predicted by these r values show a "bad" behaviour at these values of $p_x^{\pi^0}$ (see Figs. 1, 2, and 3). One could think of this second method as a rough proof of possibility (i).

We can now return to the computation of $\bar{n}_h^{t,a}(p_3)$. To derive an expression for the multiplicity associated with a hard process, we refer to Fig. 4. The hard process multiplicity is supposed to be given¹⁵⁾ by the sum of the multiplicities from the jets and the remaining multiplicity $\bar{n}_R^{t,a}$:

$$\bar{m}_h^{t,a}(p_3) = \bar{m}_R^{t,a}(p_3) + \bar{m}_{jet}^{t,a}(p_3) \quad (8)$$

In the next section we will discuss $\bar{n}_R^{t,a}(p_3)$ and we will now give an expression for $\bar{n}_{jet}^{t,a}(p_3)$.

It has been shown¹³⁾ that when a jet of transverse momentum P_x fragments without bias, the number of charged hadrons having transverse momentum greater than 500 MeV/c is approximately a linear function of P_x (at least for $P_x \leq 6$ GeV/c), with a slope of about $0.5 \text{ GeV}^{-1} \cdot c$. As, when we trigger over a p_x the average of P_x is rp_x and the spread of $\langle P_x \rangle$ is not big⁸⁾, we shall take*)

$$\bar{m}_{jet}^a(p_3) = a \langle P_x \rangle = ar p_x \quad (9)$$

leaving a as a free parameter.

For the towards jet, the trigger bias makes the average charged multiplicity very small, and a naive parametrization as

$$\bar{m}_{jet}^t(p_3) = a(r-1) p_x, \quad (10)$$

*) The linearity of \bar{n}^a with p_x for the highest ISR energy (Fig. 2) could be taken as an empirical support of Eq. (9) because of the expected near-independence of \bar{n}_R^a on $p_x^{\pi^0}$ when \sqrt{s} is big enough. As a possible intercept different from zero in Eq. (9) will be added to the intercept of \bar{n}_R^a , this possibility will be taken into account later (Section 3).

where $(r-1)p_x$ is the average remaining momentum on the trigger jet, is in good agreement with the estimate of Ref. 13.

3. SOFT AND BACKGROUND MULTIPLICITIES AND QUALITATIVE UNDERSTANDING OF THE PSB DATA

The PSB data¹²⁾ (Figs. 1, 2, and 3) have been normalized to the associated charged multiplicity for $0 \leq p_x^{\pi^0} \leq 0.5$ GeV/c. If we assume, as is normal, that in this p_T region the collision is dominantly soft, the multiperipheral model suggests¹⁶⁾ that the multiplicity associated with $p_x^{\pi^0}$ should depend only on the missing mass M_X . The M_X^2 dependence in the multiperipheral model is approximately logarithmic ($b + c \ln M_X^2$) with c close to unity¹⁷⁾. This parametrization has been shown¹⁸⁾ to give a rather good description of the charged multiplicity associated with the inclusive production of a small p_T hadron.

Therefore, to evaluate the soft charged multiplicity in each hemisphere $\bar{n}_s^{t,a}(p_3)$ we shall write,

$$\bar{m}_s^a(p_3) = b_a + \frac{c}{2} \ln M_X^2 \quad (11)$$

$$\bar{m}_s^t(p_3) = b_t + \frac{c}{2} \ln M_X^2 \quad (12)$$

(M_X^2 in GeV^2) both with the same c (to impose the asymptotic equality of both multiplicities) but possibly different b_a and b_t ; this because of the presumably different correlations between the trigger and other charged particles in each hemisphere. As we do not know any reason for putting $b_a = b_t$, we leave both parameters free, principally to emphasize this "theoretical" situation: the PSB data are not really sensitive to this difference. However, we know that c must be ~ 1.3 , which is (for instance) the value found by the CHLM Collaboration in Ref. 18. To be consistent we fix c to this value.

Let us turn now to the hard collision and give an estimate of the background multiplicity.

It is generally believed¹⁹⁾ that the asymptotic multiplicity in a given system of particles (produced coherently) is determined principally by the available energy, so we assume that the remaining particles should have a multiplicity depending on the missing mass of the background M_B in the same way as \bar{n}_s depends on M_X^2 :

$$\bar{m}_R = b' + c \ln M_B^2 \quad (13)$$

Of course there is no reason to have $b' = b$.

The value of M_B depends on the energy taken by the jets. As we shall see at the end of this section, the PSB data could suggest that the threshold energy for the production of jets is perceptibly larger than the naive evaluation $2p_x^{\pi^0}$. But this fact is more evident in the CERN-SFM data⁵⁾ (see Fig. 5)*); they study the distribution of the absolute value of the rapidity for fast charged particles ($1.1 \leq p_x \leq 1.7$) in the hemisphere opposite to the π^0 at $\sqrt{s} = 53$ GeV. They find a rather flat distribution, incompatible with a threshold energy equal to $2p_x^{\pi^0}$ (which corresponds to rapidity zero; the centre of mass of the jets coinciding with the over-all centre of mass). Although the details of this data are difficult to interpret**, in order to obtain some information from them about M_B , we are going to assume any constituent or parton model²¹⁾. So we have

$$M_B^2 \approx (1 - x_1)(1 - x_2)s,$$

where x_1 and x_2 (see Fig. 4) are the fractions of the proton momenta taken by the constituents. After some straightforward calculations we obtain^{21,22)}

$$M_B^2 \approx s - 2 P_x (\cosh \eta_2 + 1) (\sqrt{s} - P_x), \quad (14)$$

where we have taken η_1 (rapidity of the trigger-jet) equal to zero, neglecting differences between the rapidity of the trigger and the toward jet. The η_2 is the rapidity of an individual jet on the away hemisphere with transverse momentum equal to P_x [we take $\eta = -\ln(\text{tg } \frac{1}{2}\theta)$].

But, in fact, in the two-jet picture we are using, the jets are averaged over possible different masses and quantum numbers, and over the motion of the centre of mass of the jets in the over-all system (the lab. system). Then, in order to calculate the energy taken by the away side jet, we are going to compute the average η_2 rapidity from the distribution of Fig. 5. Other possibilities go beyond the scope of this work (see, for example, the last note) and will require a better approximation than formula (14), which is not a good one for θ_2 close to 0° or 180° .

To evaluate the P_x dependence of $\langle \eta_2 \rangle$ we are first going to assign the average η_2 's, corresponding to $2.0 \leq p_x^{\pi^0} \leq 2.4$ and $2.7 \leq p_x^{\pi^0} \leq 4.1$, to the average $p_x^{\pi^0}$ values in these two ranges. Then we will fit a straight line to these two values.

*) We thank P.V. Landshoff for having called our attention to this figure.

***) Is the rapidity distribution of the individual jets in the away hemisphere close to the distribution of charged particles? Do we have the same individual jets when $\eta \approx 3$ as when $\eta \approx 0$? These and other related questions must be analysed in the future^{13,20)}.

The average $\langle p_x^{\pi^0} \rangle$ in the first range turns out to be about 2.2 and in the second range about 3.0. These values are found weighting each p_x with the function $1/p_x^9$. To give an estimate of the bias introduced by the trigger and the opposite fast charged particles¹³⁾, we will multiply these numbers by 1.2 to obtain $\langle P_x \rangle$. The average η_2 's are about 1.3 for $\langle P_x \rangle \approx 2.6$ and about 1.0 for $\langle P_x \rangle \approx 3.6$. Then any straight line, $\eta_2 = I - SP_x$, reproducing approximately these values (we have tried with $2.0 \leq I \leq 2.2$, $0.30 \leq S \leq 0.37$) can be used to evaluate M_B^2 using formula (14). In Figs. 1, 2, and 3 we have used the central values of these ranges ($I = 2.1$, $S = 0.335$), but any other value in these ranges will give almost no difference.

Now we can write,

$$\bar{m}_R^a = b'_a + \frac{c}{2} \ln M_B^2 \quad (15)$$

$$\bar{m}_R^t = b'_t + \frac{c}{2} \ln M_B^2 \quad (16)$$

We leave $b'_a \neq b'_t$ because of several effects. To begin with, in Eq. (9) we have neglected an intercept which will be added to the \bar{n}_R^a intercept in writing \bar{n}_h^a [see Eq. (8)]. But there are also other causes. As has been pointed out by Combridge²³⁾, the trigger favours events in which the constituents participating in the hard scattering have their initial small transverse momenta, relative to the parent protons, in the direction of the trigger, because in these events the transverse momentum is less than the trigger p_x . Thus the residual hadronic reaction has on the average a net transverse momentum away from the trigger and one would expect b'_a larger than b'_t . However, the possible slow particles in the away jet could be seen in the toward hemisphere because of the same causes (or not detected at all if $|\vec{p}|_{lab}$ is too small). It would be difficult to know which are the more important effects. More details of this kind of trigger bias can be found in Ref. 22, but, in any case, it is clear, as happened in Eqs. (11) and (12), that there is no "theoretical" reason to impose $b'_a = b'_t$. Therefore we shall leave both parameters free, but, here also, the PSB data do not require it.

Summarizing we can write:

$$\bar{m}_s^a = b_a + 0.65 \ln M_x^2 \quad (17)$$

$$\bar{m}_s^t = b_t + 0.65 \ln M_x^2 \quad (18)$$

$$\bar{m}_h^a = \frac{b'}{a} + 0.65 \ln M_B^2 + a r p_x^{\pi^0} \quad (19)$$

$$\bar{m}_h^t = \frac{b'}{t} + 0.65 \ln M_B^2 + a(r-1) p_x^{\pi^0} \quad (20)$$

Now we must decide where the hard multiplicities (19) and (20) are dominant. To do this we look at Fig. 3. We can see that at $p_x^{\pi^0} = 0.75$ GeV/c there is a sharp change in the normalized multiplicity at $\sqrt{s} = 23$ GeV which tends to disappear with increasing energy. This sharp change could suggest a threshold energy for the creation of jets whose effect becomes smaller with increasing energy. If so, we could understand the energy behaviour of Fig. 3 for $p_x^{\pi^0} \sim 1$ GeV/c.

This kind of sharp change in the multiplicity could well be one of the effects when going from soft to hard dynamics²⁴⁾. If this would be true, it will be a useful piece of information to know where is the transition from one dynamics to the other. In contrast, it is intrinsically difficult to differentiate between an exponential and a power law for the inclusive cross-section in a small p_T range. (It could be dangerous to infer where such transition is, only from inclusive cross-section data.) In any case, the almost exact coincidence of the $p_x^{\pi^0}$ value for which the sharp change of multiplicity happens, with the p_T value (~ 0.85 GeV/c) for which the British-Scandinavian Collaboration²⁾ finds a hard parametrization already working [for $E(d\sigma/d\bar{p})(pp \rightarrow \pi^+ X)$], supports our assumption that in $pp \rightarrow \pi^0 X$ at $p_x^{\pi^0} = 0.75$ GeV/c the hard dynamics is already dominant.

Therefore we will write,

$$\bar{n}^{t,a}(p_x^{\pi^0} \approx 0.25 \text{ GeV/c}) = \bar{n}_s^{t,a}(p_x^{\pi^0} \approx 0.25 \text{ GeV/c})$$

$$\bar{n}^{t,a}(p_x^{\pi^0} \geq 0.75 \text{ GeV/c}) = \bar{n}_h^{t,a}(p_x^{\pi^0} \geq 0.75 \text{ GeV/c})$$

neglecting possible soft contributions for $p_x^{\pi^0} \geq 0.75$ GeV/c.

Then Fig. 3 is very well understood. At $\sqrt{s} = 23$ GeV, after the sharp change at $p_x^{\pi^0} \approx 1$ GeV/c, the shape is dominated by the behaviour of $\ln M_B^2$ [see Eq. (20)] because, as $r-1$ is very small (~ 0.03 when $p_x^{\pi^0}$ is far from $p_x^{\pi^0} = 1$), the last term of Eq. (19) is negligible.

As \sqrt{s} increases, the effect of the threshold energy becomes smaller, and simultaneously the term $a(r-1)p_x^{\pi^0}$ begins to compensate for the decrease due to $\ln M_B^2$. When $\sqrt{s} = 62$ GeV the threshold effect has almost faded away and, as $r-1 \sim 0.15$, the linear term of Eq. (20) begins to cancel (or even dominate) the decrease due to $\ln M_B^2$.

Also (see Fig. 2) we can arrive at the conclusion that the near equality of the *normalized* slopes can be very easily understood as a combined effect of the increase of r with \sqrt{s} and the diminished influence of the threshold energy when \sqrt{s} increases.

The quantitative study of these data will be done in the next section which, incidentally, will allow us to determine a value of a that is possibly more realistic than the one obtained by a more naive study of the PSB data.

4. COMPARISON OF OUR ANALYSIS WITH THE PSB DATA

To compare our picture with the PSB data, we have fitted to these data the unknown parameters. We consider c (~ 1.3) and r (given by Table 1 or 3) known, and M_B [see formula (14)] obtained as explained in Section 3. Similarly, we could have fixed a at about $0.5 \text{ GeV}^{-1} \cdot c$ and the description of these data would also have been adequate, but we consider it more interesting to profit from our picture to evaluate this parameter.

The parameter values obtained from the fits are^{*)}:

i) for r given by Table 1,

$$b_a = 0.05, \quad b_t = 0.25, \quad b'_a = 0, \quad b'_t = 0.17,$$

$$a = 0.56 \text{ GeV}^{-1} \cdot c$$

ii) for r given by Table 3,

$$b_a = 0.13, \quad b_t = 0.41, \quad b'_a = 0, \quad b'_t = 0.24$$

$$a = 0.56 \text{ GeV}^{-1} \cdot c$$

The curves in Figs. 1, 2, and 3 correspond to these parameters.

In these fits the value of a is fairly tightly constrained by data, but this is not the case for the b 's (see the discussion about the b parameters in Section 3). Note that the number of charged particles per GeV of the trigger in the away jet is $a \cdot r$.

5. DISCUSSION AND CONCLUSION

In the present work, we have investigated the possibility that the concept of hard scattering, which has been applied to high- p_T cross-section and correlation data by many authors, may have interesting and observable consequences for the associated multiplicity. We have studied whether the p_T and \sqrt{s} behaviour of the PSB multiplicity data in both hemispheres can be attributed to the onset of hard scattering, and have found that such an interpretation is consistent with experiment.

*) If our estimate of c (~ 1.3) would be changed by a factor, this same factor would affect the b parameters and the parameter a (recall that we are working with normalized data).

It must be noted that our two-jet picture fits the correlations and cross-section data as well, which is an important constraint on our approach.

At the present stage, our parametrization gives a particular description of our picture without specifying all the details. For instance, the motion of the centre of mass of our jets in the over-all system is averaged, and we have neglected the possible soft contributions for $p_T \sim 1$ GeV/c and the surely small hard contributions for $p_T < 0.5$ GeV/c.

A test of our model would be the observation in $pp \rightarrow \pi X$ at $p_T \sim 1$ GeV/c of all the hard production features *and an increase with p_T of the associated multiplicity in the toward hemisphere for values of the rapidity close to the trigger rapidity*. For energies big enough, our expression (20) would predict an increase with p_T of the multiplicity of the toward hemisphere.

According to our picture, changes in the invariant cross-section occur in the transition from soft to hard scattering (the changes from exponential to power-law behaviour). On the other hand, changes in the behaviour of the associated multiplicity may be one of the sharpest signals of a fundamental transition in the dynamics of particle production.

Acknowledgements

We are indebted to R. Tarrach and A.C.D. Wright for several discussions, and to P.V. Landshoff and M. Le Bellac for critical comments and a careful reading of the manuscript. One of us (A.C.) acknowledges the hospitality of the CERN Theoretical Study Division and the financial support of GIFT.

REFERENCES

- 1) Aachen-CERN-Heidelberg-Munich Collaboration: K. Eggert et al., Nuclear Phys. B98, 49 and 73 (1975).
- 2) British-Scandinavian Collaboration: B. Alper et al., Nuclear Phys. B100, 237 (1975).
- 3) CERN-Collège de France-Heidelberg-Karlsruhe Collaboration: M. Della Negra et al., Nuclear Phys. B104, 365 (1976).
- 4) CERN-Columbia-Rockefeller-Saclay Collaboration: F.W. Büsser et al., Nuclear Phys. B106, 1 (1976).
- 5) CERN Split-Field Magnet experiment 412: P. Darriulat et al., Nuclear Phys. B107, 429 (1976).
- 6) Daresbury-Liverpool-Rutherford Collaboration: B. Alper et al., Rutherford Preprint RL 76-031 (1976).
- 7) Pisa-Stony Brook Collaboration: see P.V. Landshoff, Ref. 11.
- 8) S.D. Ellis, M. Jacob and P.V. Landshoff, Nuclear Phys. B108, 93 (1976).
- 9) J.D. Bjorken, Lectures at 1975 SLAC Summer Institute.
- 10) G. Preparata and G. Rossi, preprint CERN TH.2163 (1976).
- 11) For a discussion of hard-scattering models, see the reviews of:
S.D. Ellis and R. Thun, CERN TH.1874;
S.D. Ellis *in* Proc. 17th Internat. Conf. on High-Energy Physics, London, 1974 (Science Research Council, Rutherford Lab., Didcot, 1974), p. V-23;
P.V. Landshoff, *ibid.*, p. V-57;
D. Sivers, R. Blankenbecler and S.J. Brodsky, Phys. Reports 23, 1 (1976).
- 12) T. del Prete, Invited talk at the 9th Balaton Symposium on Particle Physics, Balatonfured (Hungary), 1974; CERN preprint.
- 13) M. Jacob and P.V. Landshoff, preprint CERN TH.2182 (1976).
- 14) R. Blankenbecler, S.J. Brodsky and J.F. Gunion, Phys. Letters 39B, 649 (1972).
R. Blankenbecler and S.J. Brodsky, Phys. Rev. D 10, 2973 (1974). See also Sivers et al., Ref. 11.
- 15) As an example of this kind of picture, see J.L. Alonso and A.C.D. Wright, Phys. Rev. D 12, 776 (1975). The same kind of ideas have been used by the PSB Collaboration (see Ref. 7).
- 16) C.F. Chan and F.C. Winkelman, Phys. Rev. D 10, 3645 (1974).
- 17) W.R. Frazer et al., Rev. Mod. Phys. 44, 284 (1972).
G.F. Chew and A. Pignotti, Phys. Rev. 176, 2112 (1968).
- 18) See J.L. Alonso and A.C.D. Wright (Ref. 15) and references therein. Also the CHLM Collaboration: M.G. Albrow et al., Nuclear Phys. B102, 275 (1976).
- 19) See, for instance, E.L. Berger *in* Proc. Ecole d'Eté de Physique des Particules, Gif-sur-Yvette, 1973 (IN2P3, 11 rue Pierre et Marie Curie, 75005 Paris).

- 20) R. Raitio and G. Ringland, SLAC-PUB-1620 (1976).
- 21) S.M. Berman, J.D. Bjorken and J.B. Kogut, Phys. Rev. D 4, 3388 (1971).
R. Blankenbecler, S.J. Brodsky and J.F. Gunion (see Ref. 14).
P.V. Landshoff and J.C. Polkinghorne; Phys. Letters 45B, 361 (1973).
S.D. Ellis and M.B. Kislinger, Phys. Rev. D 9, 2027 (1974).
- 22) J.D. Bjorken, Phys. Rev. D 8, 4098 (1973).
- 23) B.L. Combridge, Phys. Rev. D 12, 2893 (1975).
- 24) This possibility has been emphasized by J.L. Alonso and A.C.D. Wright (Ref. 15).

Table 1 (r values)

\sqrt{s} (GeV)	n	r
23	12	1.033
31	11	1.046
45	10	1.067
53	9	1.100
63	8	1.158

Table 2

\sqrt{s} (GeV)	N	F	M	χ^2 per point
23	4.5	11.4	1.70	0.5
31	3.03	16.0	1.20	1.3
45	3.10	10.6	0.5	0.7
53	3.10	11.4	0.04	0.7
63	3.07	14.8	0.62	0.3

Table 3 [r values^{*)}]

π^0 p_x (GeV/c) \ / \sqrt{s} (GeV)	23	31	45	53	63
1.25	1.25	1.29	1.28	1.24	1.32
1.75	1.11	1.15	1.20	1.20	1.23
2.25	1.06	1.09	1.16	1.16	1.18
2.75	1.03	1.06	1.13	1.14	1.14
3.25	1.02	1.04	1.10	1.11	1.12
3.75	1.02	1.03	1.09	1.10	1.10
4.25	1.01	1.02	1.07	1.08	1.08

*) As $p_x^{\pi^0} = 0.75$ GeV/c is below the p_x value for which we have assumed scaling [and below the p_T values of the data used to fit formula (3)], we shall take for it the same r value as for $p_x^{\pi^0} = 1.25$ GeV/c. Discussions (i) and (ii) of Section 2 support this choice.

Figure captions

- Fig. 1 : Normalized average total multiplicity of charged particles at $\sqrt{s} = 23, 31, 45, 53, \text{ and } 63 \text{ GeV}$ as a function of p_T of π^0 at $\theta_{\text{cm}} = 90^\circ$. The dashed lines are our computation with r taken from Table 1, and the solid lines are the results from Table 3.
- Fig. 2 : Normalized partial multiplicities of charged particles in the hemisphere away from the detected π^0 , plotted as in Fig. 1. Solid and dashed lines as in Fig. 1.
- Fig. 3 : As Fig. 2 but in the toward hemisphere from the detected π^0 .
- Fig. 4 : Momentum diagram of a hard scattering collision.
- Fig. 5 : Distribution of the absolute value of the rapidity for charged particles in the hemisphere opposite the π^0 at $\sqrt{s} = 53 \text{ GeV}$. The data (Ref. 5) are broken into two $p_x^{\pi^0}$ intervals and summed over charged particles for $1.1 < p_x < 1.7 \text{ GeV}/c$. The dashed-dotted line indicates the mean particle density from minimum bias events, and the solid lines the assumed η distribution used to calculate the average η_2 value.

NORMALIZED TOTAL MULTIPLICITY

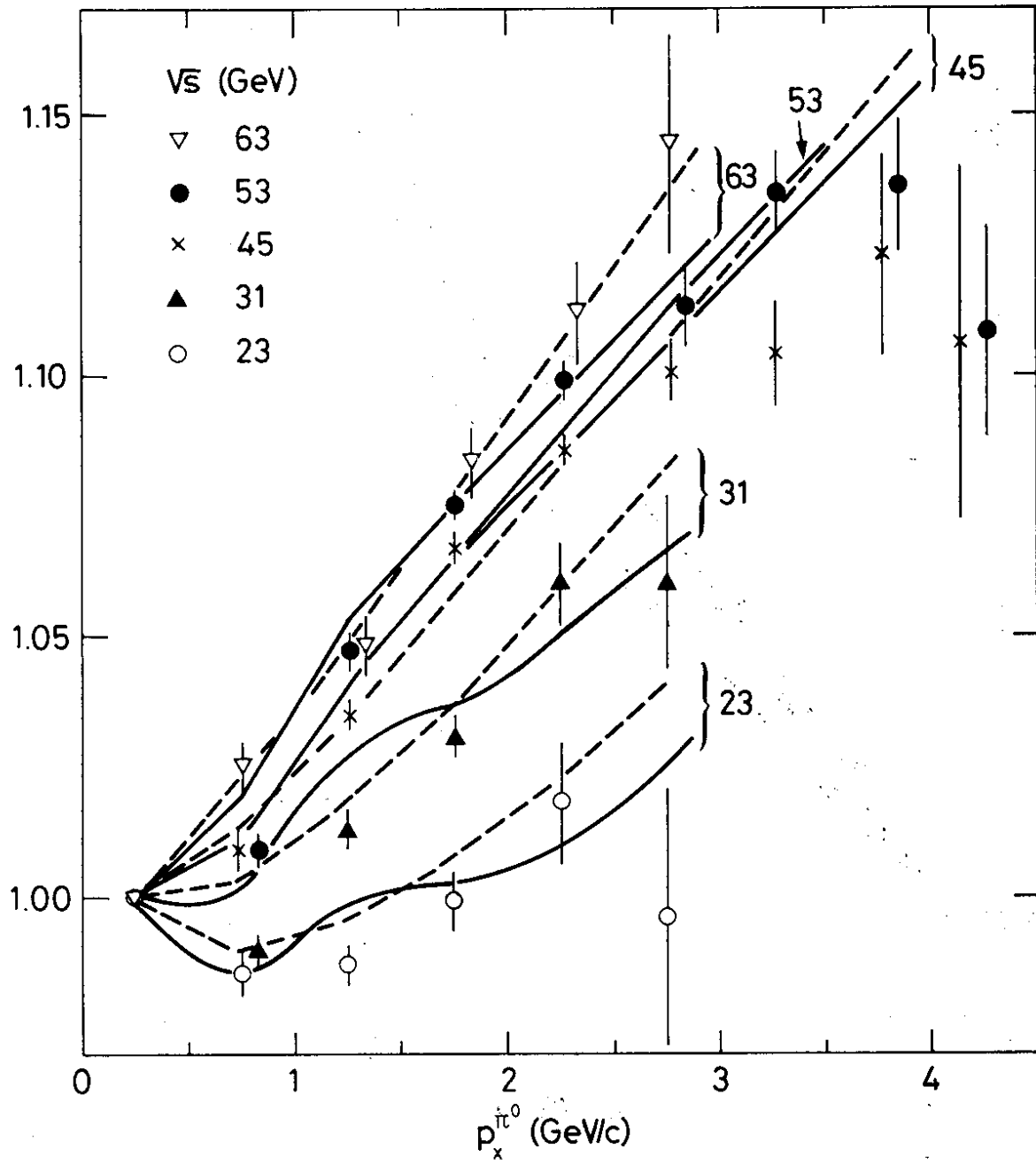


Fig. 1

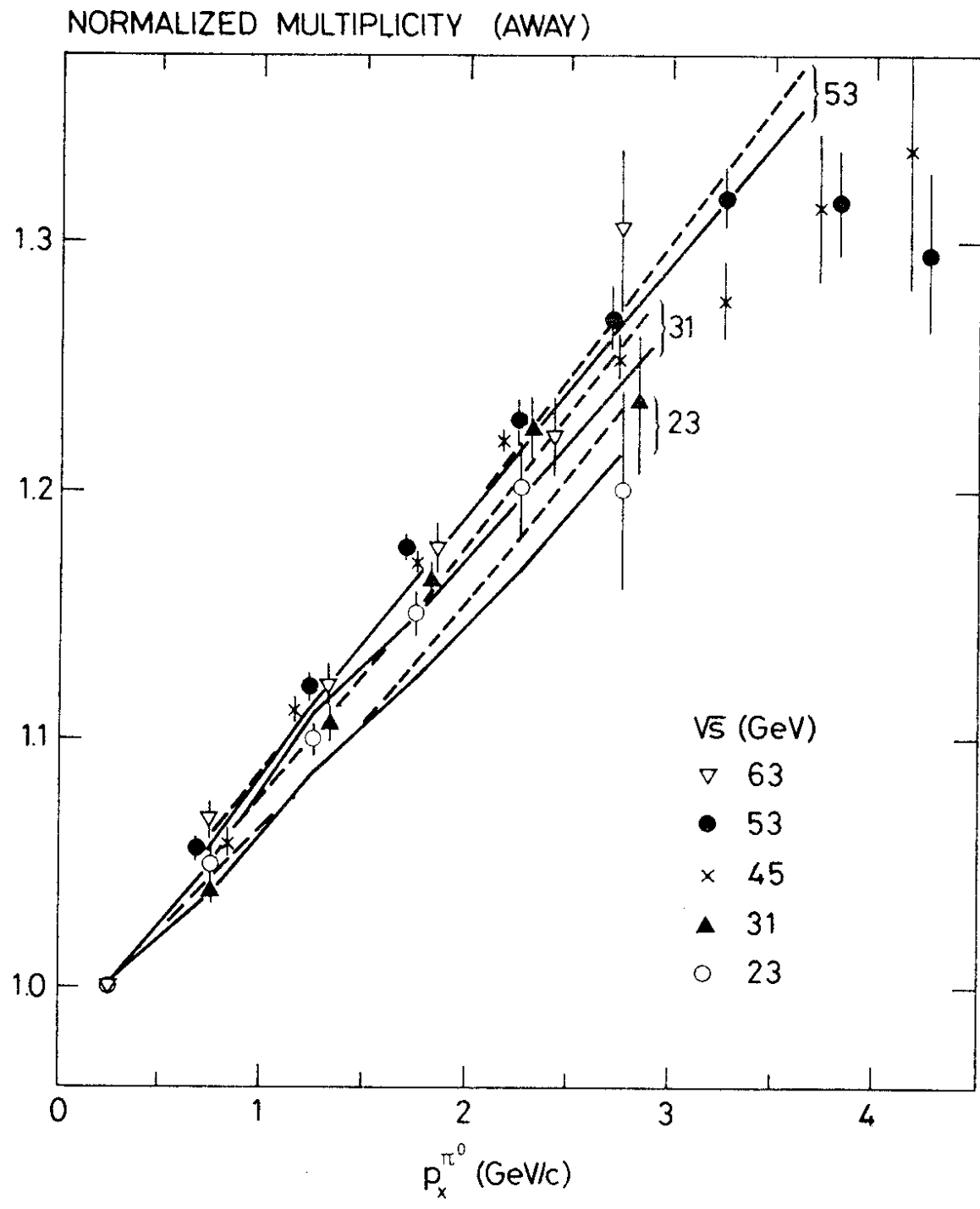


Fig. 2

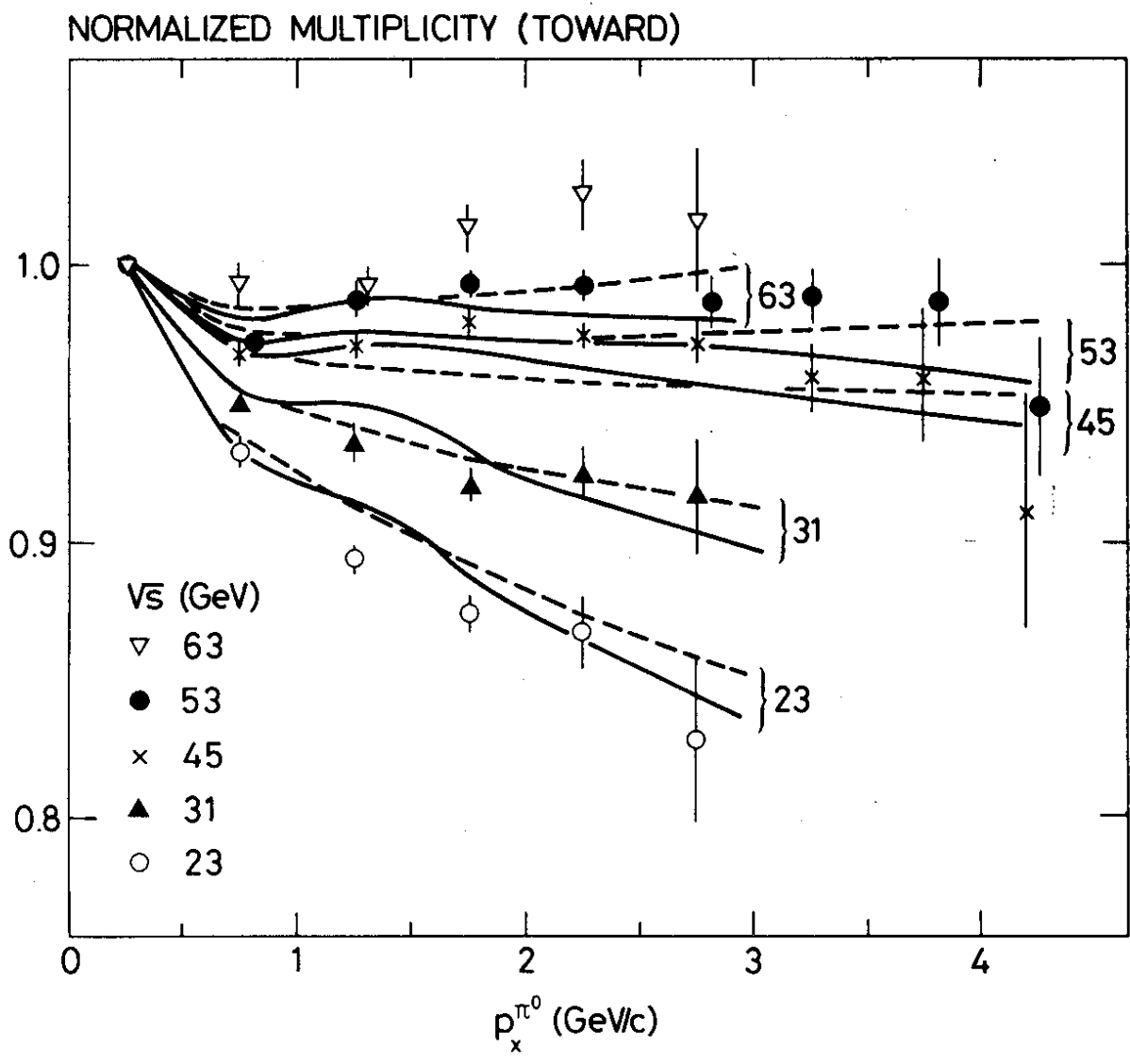


Fig. 3

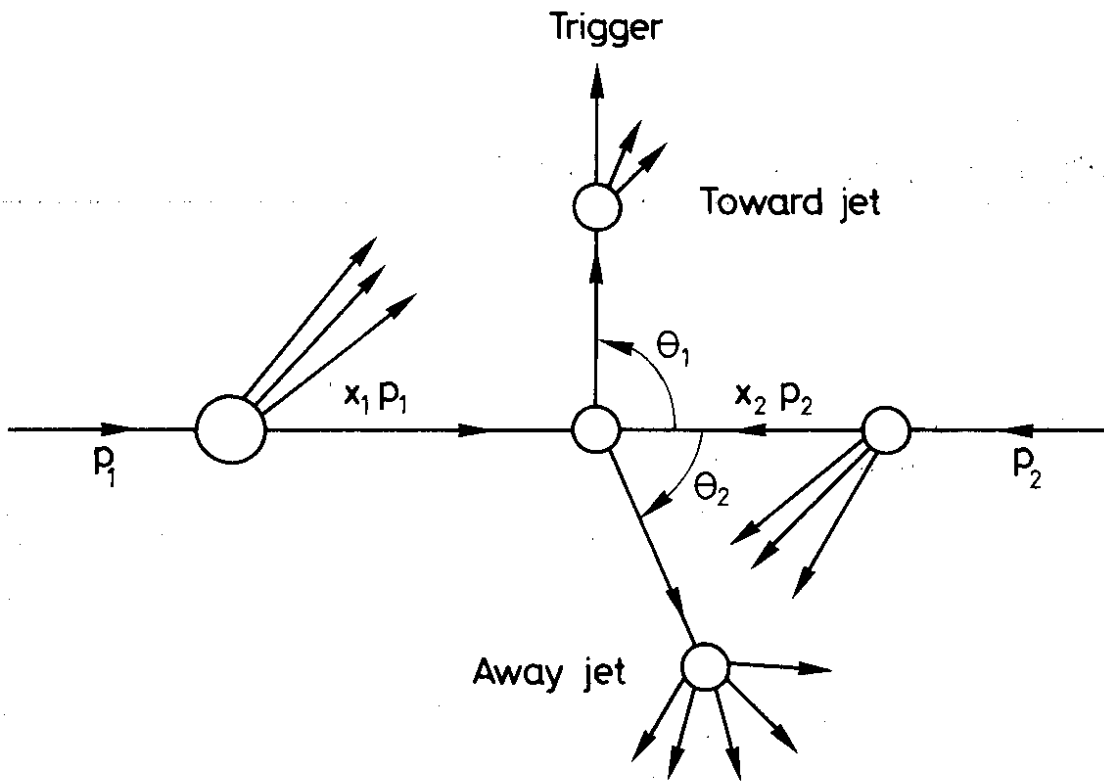


Fig. 4

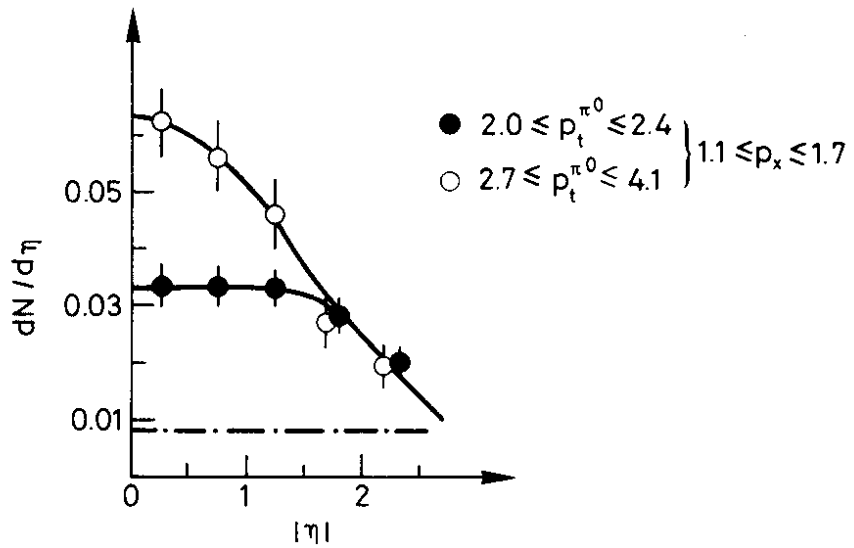


Fig. 5